Original Paper

MEASUREMENT AND CONTROL

Measurement and Control
1–19

DOI: 10.1177/0020294018801382
journals.sagepub.com/home/mac
SAGE

Challenges in improving the performance of eddy current testing: Review

Ahmed N AbdAlla[1], Moneer A Faraj[2], Fahmi Samsuri[2], Damhuji Rifai[3], Kharudin Ali[3] and Y. Al-Douri[4]

Abstract

Eddy current testing plays an important role in numerous industries, particularly in material coating, nuclear and oil and gas. However, the eddy current testing technique still needs to focus on the details of probe structure and its application. This paper presents an overview of eddy current testing technique and the probe structure design factors that affect the accuracy of crack detection. The first part focuses on the development of different types of eddy current testing probes and their advantages and disadvantages. A review of previous studies that examined testing samples, eddy current testing probe structures and a review of factors contributing to eddy current signals is also presented. The second part mainly comprised an in-depth discussion of the lift-off effect with particular consideration of ensuring that defects are correctly measured, and the eddy current testing probes are optimized. Finally, a comprehensive review of previous studies on the application of intelligent eddy current testing crack detection in non destructive eddy current testing is presented.

Keywords

Eddy current testing, non destructive testing, lift-off, defect detection

Date received: 13 May 2018; accepted: 22 August 2018

Introduction

Pipelines are regarded as a preferable way of transporting oil, refined oil products or natural gas in large quantities over land. The network of pipes has advantages over other means of transportation (such as train/truck) because of its high cost.[1,2] Thus, it is essential to continuously check the conditions of the pipeline on a regular basis.

The eddy current testing (ECT) method has long been utilized for nondestructive testing (NDT)[3] and widely applied to inspect conductive material structure in order to identify their structural integrity. Betta et al.[4] suggested that coils be used to detect the magnetic field (MF) as the primary indicator of a crack in the pipeline. However, this method is limited due to poor sensitivity at low frequency for the inspection of the subsurface defect, and thickness of materials demands sensitivity at low frequency. To overcome the poor-sensitivity limitation of the traditional eddy current probe, NDT technology has the advantage of employing magnetometer (MR) sensors to obtain maximum information from the component being tested.[5]

Many types of research have introduced many structures of ECT for the purpose of material inspection. Lee et al.[6] proposed that the bobbin coil is used to induce the eddy current in small piping, and the MF can be picked up by utilizing a Hall sensor array. This technique allows the distribution of the distorted electromagnetic (EM) field around outside diameter of the stress corrosion cracking so it can be imaged without the need for a rotating apparatus. In another study, Postolache et al.[7] proposed two rectangular planar excitation coils and an array of five AA002 giant magneto resistive (GMR) sensors for defect detection of an aluminum plate. They found that the optimization of the ECT probe had enhanced the ability of inspection with rapid scanning time.

Ye et al.[8] used a pair of orthogonal (axial and circumferential) coils to generate an eddy current in steam

[1]Faculty of Electronic and Information Engineering, Huaiyin Institute of Technology, Huai'an, China
[2]Faculty of Electrical & Electronics Engineering, University Malaysia Pahang, Pekan, Malaysia
[3]Faculty of Electrical & Automation Engineering Technology, TATI University College, Kemaman, Malaysia
[4]Nanotechnology and Catalysis Research Center (NANOCAT), University of Malaya, 50603 Kuala Lumpur, Malaysia

Corresponding author:
Ahmed N AbdAlla, Faculty of Electronic and Information Engineering, Huaiyin Institute of Technology, Huai'an 223002, China.
Email: dramaidecn@gmail.com

generator tube wall and a GMR array to detect the induced MF. The probe showed superior inspection accuracy and sensitivity to defects of the axial and circumferential directions. Zeng et al.[9] suggested a multi-line as an excitation coil, while a GMR sensor could be placed on the line of symmetry to detect any changes in the MF. The simulation result shows improvement in the detection sensitivity for multilayer subsurface flaws.

Rifai et al.[10] also described the application of GMR sensors in ECT. Also discussed in detail were the limitation of utilizing the coil as a sensor and compensation techniques that have been used in the ECT. In another study, Ali et al.[11] discussed in detail the method of the ECT and the parameters that impacted the signal fundamental in relation to the hardware and software. García-Martín et al.[12] delibertated an overview of the primary variables and the principles of ECT sensors.

Therefore, the structure of the ECT probe should be identified to provide and evaluate the tested materials without destroying them.[13] This paper will review the eddy current probe structure and error compensation of the eddy current probes to obtain the ideal measuring depth of defect on carbon steel pipeline. The lift-off effect will be discussed in detail to ensure that the measuring defect is right. This study will also introduce different conventional and intelligently lift-off compensations.

The principle of ECT

The diagram illustrating the operation principle of the ECT is shown in Figure 1. According to Faraday's law, the driving coil is excited to produce a MF, known as eddy currents.[14–16] The emf induced in the receiving coils are generated by the eddy currents.

Four steps can demonstrate the MF connection between the primary and secondary coils:

- Alternating current through the coil produced by the principal MF.
- Alternating primary MF produces the EC in the conductive sample.
- EC produces a secondary MF in an opposing direction.
- Flaws in the sample perturb the EC and decrease the secondary MF, which results in the variation of impedance changes of the coil.

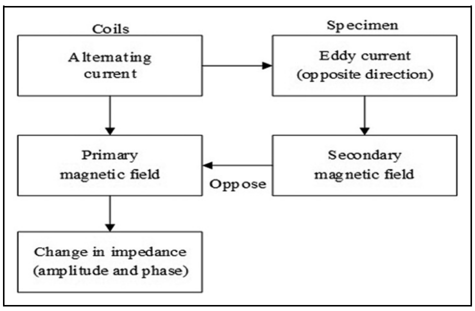

Figure 1. Principle for the eddy current testing operation.

The advantages of ECT include the fact that they are economical and environmentally friendly as a non-contact method with high detectability, inspection speeds and offers good discrimination. On the other hand, the main disadvantages are it is sensitive to defects near the surface and is only applicable to conductive materials.[12,17]

Eddy current probe

Various configurations are presented for the excitation source and detection sensor. However, in many in-service applications, the inductive coils are utilized both as a field source and field sensors. As a result, the eddy current probes are commonly classified according to their configuration and mode of operation. The probe configuration is closely related to the way the coil or coils' connection covers the testing area of interest. The probe operation mode is commonly classified into reflection, differential, absolute and hybrid modes, whereas some of the standard configurations include the outside diameter probes, inside diameter (bobbin) probes, bolt hole probes and surface probes.[18]

An inductive probe can include one or more coils. In conventional eddy current probes, these coils typically comprise lengths of wire wound in a helical manner like a solenoid. The winding will commonly have more than one layer to increase the value of inductance. As mentioned above, there are many ways in which these coils can be constructed based on the specified application. Conventional ECTs are transmit–receive probes, multi-pancake and/or rotating pancake probes and bobbin probes. Each method has its respective strengths and weaknesses in consideration of their characteristics such as the test speed, flaw detection sensitivity and probe structure complexity.[19]

Bobbin probes

Figure 2 shows the two types of the bobbin probes which are called the differential and absolute bobbin probes. Differential bobbin probe has two coils positioned at 180° out of phase. The probe has excellent sensitivity to detect abrupt anomalies and small defects such and relatively unaffected by lift-off, pitting corrosion, fretting wear and probe wobble. However, the probe is not sensitive to metallurgical and gradual changes.[20,21]

Absolute bobbin consists of a single bobbin coil and a second identical reference coil. The second identical reference coil is used for EM shielding of the inspected tubing and electronic balancing. The probe has excellent sensitivity to detect axial cracks and is highly sensitive to material property variations and gradually varying wall thinning.[6] The main disadvantage of the absolute coil is that the defect is typically superimposed over a lift-off as the large signal.

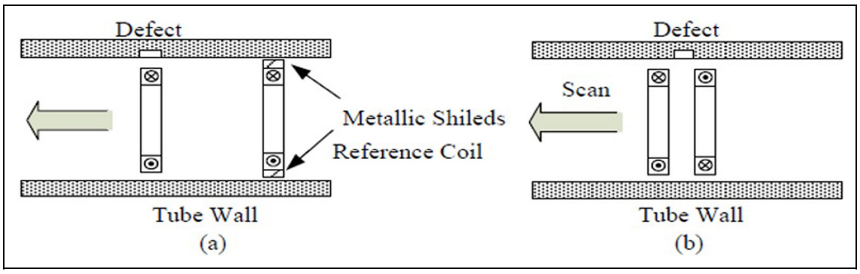

Figure 2. Tube inspection probes: (a) absolute and (b) differential.

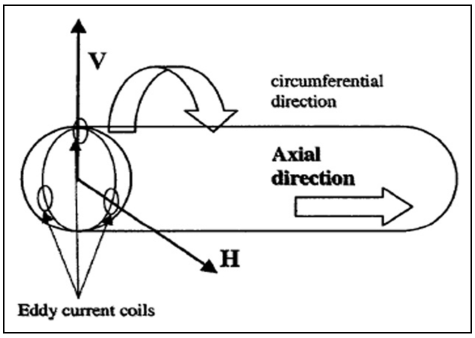

Figure 3. Rotating probe.

Rotating probes

The rotating eddy current probes are used for high-resolution imaging of the steam generator tubes as shown in Figure 3.[8,22] The rotating probe is sensitive to defects of all orientations and has a high resolution and improved sensitivity to characterize and size defects. However, the mechanical rotation of the coils causes serious wear leading to frequent probe failure and affect the inspection time, and subsequently, the cost will increase significantly.[23]

Array probe

The array probe types include the smart, probe X-probe, C-probes and intelligent probe. The array probe works as a transceiver probe and can cover the direction of 360°. The transmitting coils are actively driven by the AC source with a different range of frequencies. The receiving coils generate an induced voltage equal to the change of magnetic flux through the coil. The array probe response for different orientation defects has a higher signal-to-noise ratio (SNR) and is 10 times faster than the rotating probe. Another disadvantage is that the hand array probe is very costly because of its complicated excitation and data acquisition parts[24,25] as shown in Figure 4.

Rotating field probe with bobbin coil

Figure 5 shows the excitation part which consists of three coils with identical 120 axes degrees apart and balanced alternating currents with adjustable frequency, phase and amplitude. The rotating MF is generated without mechanical rotating support.[21,26]

Comparison of eddy current probes

The advantages and disadvantages of eddy current probes for the NDT as described in Table 1.[30]

EM NDT techniques

The EM methods of NDT comprise a full spectrum of techniques ranging from static (DC) methods to high-frequency (10 THz) methods. The next section presents the most comprehensive inspection technique that used in the EM NDT.[31]

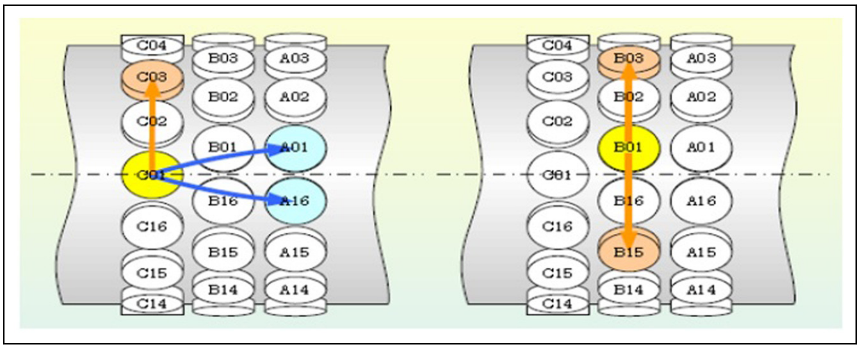

Figure 4. Array probe.

Table 1. ECT probes for tube or pipe assessment inspection.

Types	Advantages	Disadvantage
Bobbin probe[6,18]	Rapidly inspects speed, determine defect depth and length, lower price, higher dependability and toughness and sensitive to axial flaws	one dimension scan data and insensitive to circumferential defect
Rotating probe[21]	Depth C-scan visualization for inner tube surface, sensitivity to the flow of all orientations and higher SNR	Low dependability and toughness, costly and inspection speed is slow
Array probe[27,28]	Sensitivity to flaws in all directions, inspection speed is fast and size defect with the depth and length of the C-scan visualization for inner tube surface	Very expensive with complex instrumentation
Rotating field probe[8,29]	Sensitive to defects of all directions, no need rotating probe mechanically, high inspection speed	Need field test approve

SNR: signal-to-noise ratio.

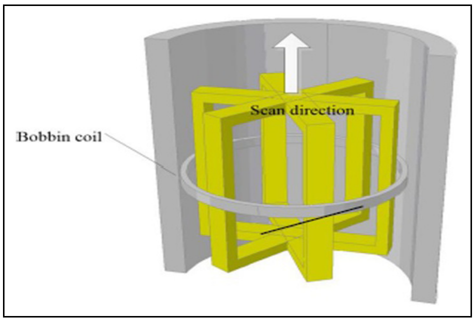

Figure 5. 3D model of rotating field probe with bobbin coil.

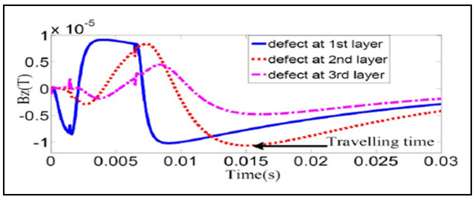

Figure 6. PEC to test multilayer sample.[33].

Pulsed eddy current

Pulsed excitation produces transient signals with a wide range of frequency components. Hence, it contains more information compared to a single-frequency excitation.[32,33] The pulsed eddy current (PEC) signals have common features in the transient characteristics such as the peak amplitude, time-to-peak amplitude and time-to-zero crossing. The peak amplitude will determine the defect size. The defect depth or material thickness will be identified by the peak amplitude.[34–36] The earliest study of PEC for crack detection in layered structures with installed fasteners was conducted by Harrison.[37,38] Giguere et al.[39] also studied the detection of cracks beneath rivet heads using the transient EC techniques. Figure 6 shows some experimental results of PEC to test multilayer sample.[33]

ECT with MF measurement method

The most recent research introduced the GMR sensor. It is widely used in many applications because the sensitivity of these sensors is independent of the MF, it has a high bandwidth, only requires a low power supply, the dimensions of GMR are small and the output signal is high compared to the other MR sensors. Therefore, the GMR-based EC testing exhibits significant advantages in detecting complex geometry such as a layered component inspection.[40] The directional property of the GMR sensor had been used to locate edge cracks in aluminum specimen.[40,41] A needle-type GMR imaging technique named the SV-GMR system was designed for the inspection of a bare polychlorinated biphenyl structure to measure the magnetic fluid density in a living body.[10,42]

High-resolution GMR elements are fabricated in a small package of sensors arrays. An inspiring application of this array probe was found in the evaluation of metal medical implants for invisible cracks.[43] A linear array of 20 GMR elements was packaged to image a hole defect in a steel plate using 1 Hz excitation. Designs of GMR array probes in identical elements had been studied to detect subsurface cracks.[44] High-density GMR arrays were especially promising for rapid scanning of a large area as well as high-resolution imaging.[7,45] Another type of GMR array sensors that use two-directional elements was investigated in the EC testing to detect surface cracks of unknown orientation. They measure both X-component and Y-component of the MF at the same point.[5] A fast Fourier transformation to enhance the ECT probe based on the GMR array sensors for pipe inspection was utilized by Du et al.[46]

The transient excitation of the coil probes with two MR sensors or two Hall sensors in differential mode have been studied by Lebrun et al.[47,48] and used for characterizing crack parameters. Kim et al.[49] introduced a method for the assessment of aircraft structures. The system produced pulse excitation that energized a planar multi-line coil. The GMR field sensor was used to detect the transient field. Tai et al.[50] studied similar transient features for an inversion scheme to qualify the conductivity and thickness of the samples. Table 2 shows the difference between the eddy

Table 2. Overviews of the utilities AC signal in eddy current testing with different probe designs.

Author	Analysis tool/ software simulation	Type of sample	Excitation coil	Sensing	Finding
D'Angelo et al.[51]	Multilayer perceptron neural network (NN)	Aluminum alloy (2024 T3)	Coil with a parallelepiped shape	GMR sensor	Mechanical rotation of EC probes around wall tube is needed to inspect the inside pipe
Zhang et al.[52]	Finite element method (FEM)	Conductive plate	Rectangular excitation coil	Cylindrical pickup coil	The analytical results agree with FEM results and the forward model of quantitative detection for ECT of multilayer conductive structure
Postolache et al.[53]	ANN/multilayer perceptron/ finite element simulation	Aluminum plate	ECP1 has a pancake type (large diameter and small height) and ECP2 has a small diameter and long length	The GMR sensor in both cases	Implementation of the NN classification method improves the dependability of defect classification
Zeng et al.[9]	Three-dimensional finite element mesh	Aluminum and steel fasteners	A multi-line coil	GMR sensor located on the line of symmetry	Simulation results establish that the proposed method improved the sensitivity of the method in detection of multilayer subsurface flaws
Yang et al.[54]	Finite element simulation/ image fusion technique	Steel fastener	Planar multi-line coil	GMR sensor installed on the line of symmetry	Eliminate the difficulty of detecting cracks under steel fasteners by using the characteristics of tangential components By and Bx of the induced magnetic field
Yang et al.[55]	FEM	Aluminum and steel rivets	Two unidirectional planar coils oriented in orthogonal directions	GMR sensor	The experimental and simulation outcomes indicate that the method can detect all orientations of a flaw under the fastener
Kim and Lee[56]	Experimental	Inconel 690 tubes	Multiple coils with three deferent angle	Multiple coils with three deferent angle	The experimental results prove that the suggested probes are more sensitive to circumferential defects and sensitive to axial defects by employing both the new probes and the conventional bobbin
Ye et al.[8]	C-scan image/ FEM	An Inconel 690 steam generator tube	Pair of orthogonal (axial and circumferential) coils	A circumferential array of 16 GMR sensors	The probe has high inspection speed and sensitivity to defects of the axial and circumferential directions. However, it has very complicated excitation and data acquisition system
Paw et al.[57]	Design of experiment software	Carbon steel pipe	Encircling coil for a differential probe (ECDP) and encircling coil for an absolute probe (ECAP)	Encircling coil for a differential probe (ECDP) and encircling coil for an absolute probe (ECAP)	The probe cannot detect the transverse defect

(Continued)

Table 2. (Continued)

Author	Analysis tool/ software simulation	Type of sample	Excitation coil	Sensing	Finding
Shim et al.[58]	The primary simulated water of a pressurized water reactor	Alloy 690 steam generator tubes	A conventional bobbin coil probe and a conventional 3-coil motorized rotating probe	A conventional bobbin coil probe and 3-coil motorized rotating probe	The general corrosion rates of alloy with different 690TT tube noises can be predicted from the tube noise value measured by a rotating pancake coil probe
Ribeiro et al.[59]	A conformal transformation	Aluminum plate	A rectangular cross coil	GMR sensor	The conformal transformation used to model the crack of an aluminum plate to preview the acquired voltage signals
Yin and Xu[60]	Peak frequencies of the sensor signal have been utilized to calculate the thickness of the plate	Aluminum plates	Triple-coil sensor measurements are made by exciting the middle coil	Triple-coil sensor measurements are made by taking induced voltages from the bottom and the top coils	The results show that the technique is highly immune to lift-off variations
Lee et al.[6]	FEM	Piping of titanium alloy	The bobbin coil	State Hall sensor array	This technique allows the distribution of the distorted EM field around outside diameter stress corrosion cracking to be imaged without the need of a rotating apparatus
Joubert et al.[61]	C-scan images	Bore hole	Bobbin coil	The row of pickup coils of the sensing array	The acquired experimental results showed a great sensing capability of the designed probe in the 10–800 kHz frequency range
Menezes et al.[62]	Numerical simulation FEM	Aluminum plate	Pancake coil	GMR sensor and a permanent magnet to put the sensor working in its linear range	The magnetic flux density is closely correlated with the crack's depths where maximum amplitude disturbance depends on the crack depth
Xie et al.[63]	FEM/the NCSF algorithm	A plate of 7075 aluminum alloy	A large uniform coil is designed on the bottom and top layers	64 sensing coil elements on two middle layers	All of the results show that the array is not just sensitive to micro cracks, however additionally able to crack length size
Suresh et al.[64]	ANSYS-based FEM	Ferro tube	Bobbin coil/core of iron	A hall sensor	The efficiency of the suggested bobbin coil is effective to inspect the small diameter tube
Ye et al.[65]	FEM	Two-layer aluminum	Two orthogonal coils	Two linear arrays of GMR sensors are located above and below the orthogonal coils	Experimental results present that the probe can detect flaws regardless of their orientation. The differential scheme reduces the effect of the background field and improves SNR

(Continued)

Table 2. (Continued)

Author	Analysis tool/ software simulation	Type of sample	Excitation coil	Sensing	Finding
Lee et al.[66]	FEM	The steel (SS400) plate	The two probes measure the current and the voltage to determine the coil impedance	A coil winding and a ferromagnetic core are used as a sensing element	A low frequency has been applied for deep internal inspection of a ferromagnetic material
Rifai et al.[67]	FEM	Carbon steel pipe	Pair of orthogonal (axial and circumferential) coil	An array of GMR sensors	It has very complicated excitation and data acquisition system
Xin et al.[21]	3D FEM	Steam generator tubes	Three identical windings located on the same physical axes 1201 apart	The response signal can be picked up by bobbin coil in the center	The probe is sensitive to flaws of all orientations in the tube wall, and the line scan data enable rapid inspection rates
Abdalla et al.[68]	Fuzzy interference system	Carbon steel pipe	Pair of orthogonal (axial and circumferential) coil	Hybrid absolute and differential probe	The Mamdani-type fuzzy use to integrated absolute and differential probe

GMR: giant magneto resistive; EC: eddy current; ECP: eddy current probe; ECT: eddy current testing; ANN: artificial neural network; NCSF: normalized crack signal fitting; SNR: signal-to-noise ratio.

current methods which rely on the sensor element that utilities alternative current signal in ECT.

Multi-frequency techniques

NDT widely uses multi-frequency techniques (MFTs). The MFT expanded the capabilities of using single-frequency testing which allows simultaneous tests.

The multi-frequency process uses a composite signal and subtracts the undesirable signal.[12] The main undesirable signal caused by changes in the temperature variation, material geometrical and probe lift-off.[69] MFTs are usually accomplished by combining the results obtained at different frequencies in the spatial domain. Liu et al.[69] presented integrate two- (multi) frequency injection with dimensional spatial domain named as a pyramid fusion method. The SNR improved due to reduction in noise sources which demonstrated the potential of signal enhancement via fusion method or raster scanning.[70] A two-dimensional (2D) surface produced changes over of the impedance or impedance by raster scanning images.[12] Image processing techniques can be applied to detect cracks using ECT. Bartels and Fisher[71] proposed a multi-frequency eddy current image processing technique for the non destructive materials evaluation. SNR improvement up to 1100% over traditional two-frequency techniques a sequence of complex valued images generated from 2D ECT to maximize the SNR. The linear combination of the images by Bartels and Fisher[71]

$$d(x, y) = \sum_{i=1}^{2N_f} c_i f_i(x, y)$$

where N_f is the number of test frequencies and f_i are extracted from the 2D images. Results on experimental data demonstrate.

Factors contributing to eddy current signals

The signal from an eddy current probe includes a collection of responses from defects, sample geometry and probe lift-off.[72,73] Therefore, it may be difficult to separate a single influence. Adequate assessment of flaws or any other surface properties is likely when other factors are understood.[7] The primary factors influencing the response of an eddy current probe are explained in this section.

Frequency

Eddy current response is strongly affected by the frequency chosen for the investigation. This factor should be appropriately selected by the operator, based on the crack detection sample such as lower frequencies for bulk characterization and higher frequencies for surface characterization.

Many authors such as Ditchburn et al.[74] and Thollon et al.[75] utilize this range, and they suggested the range of 100 Hz–10 MHz as standard inspection frequencies in ECT.[19] However, a few authors such as Owston[76] characterized high frequency at 25 MHz for thin metallic coatings and detecting surface defects. In the inspection of ferromagnetic materials, low-frequency tests are applied to penetrate into the test specimen and compensate for their high permeability.

Table 3. Typical depths of penetration.

Metals	36.8% δ				
	1 kHz	4 kHz	16 kHz	64 kHz	256 kHz
Copper	0.082	0.041	0.021	0.010	0.005
Uranium	0.334	0.167	0.084	0.042	0.021
Zirconium	0.516	0.258	0.129	0.065	0.032
7075 T-6	0.144	0.072	0.036	0.018	0.009
Steel	0.019	0.009	0.0048	0.0024	0.0012
6061 T-6	0.126	0.063	0.032	0.016	0.008
Magnesium	0.134	0.067	0.034	0.017	0.008

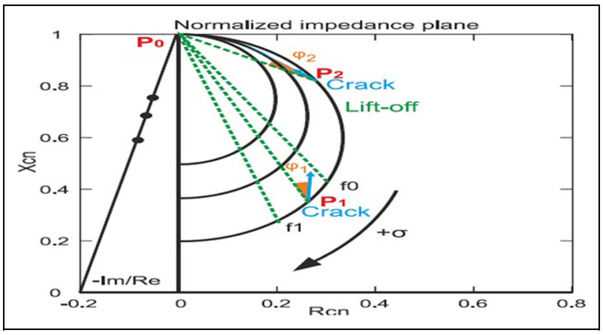

Figure 7. Lift-off curves and crack displacement at impedance plane.[82]

Table 4. Conductivity and resistivity of conductive materials.

Material	Conductivity (% IACS)
Copper	100.00
Gold	70.00
Aluminum 6061	42.00
Brass	28.00
Copper-nickel 90–10	9.10
Cast steel	10.70
Inconel 600	1.72
Silver	105.00
Stainless steel 304	2.39
Zircalloy-2	2.40

Ramos et al.[77] have studied the detection of subsurface flaws relating to the characterization of depth profiles of the subsurface defects in aluminum plates.[78] However, the high frequency applied for the inspection of small discontinuities occured in the near-surface.[79,80] Table 3 summarizes the impact of different frequency values on the depth of penetration of several materials.[81]

Conductivity of test material

Electrical conductivity and the magnetic permeability of the test objects of the material depend on the microstructure, for example, grain structure, the presence of a second phase, work hardening and heat treatment. Greater conductivity of a material such as copper and aluminum will lead to greater flow of the eddy currents and hence the probe coil resistance.

In great conductive materials, defects or cracks produce a high signal as an impedance plane, as illustrated in Figure 8. Furthermore, the phase lag between the lift-off line and the defect is $\phi 1 > \phi 2$,[82] which is significant, as indicated in Figure 7.

However, the penetration depth of highly conductive materials at a fixed frequency is lower than in lower conductive materials such as stainless steel and steel. The conductivity of the different materials can be measured using the International Annealed Copper Standard (IACS). Table 4 summarizes the conductivity of common elements.[83]

Magnetic permeability

ECT signals are significantly affected by ferromagnetic materials due to the increase in flux produced by the significant relative permeability of certain materials such as stainless steel or carbon steel.[84] The permeability of material changes the coupling of the coil with the conductive specimen and subsequently affects the reactance of the coil. Permeability has a significant effect on the ECT compared to conductivity, where the crack detection has no potential when permeability changes randomly.[85,86]

Lift-off

ECT is strongly affected by the amount of lift-off which can be defined as the separation distance between the excitation coil surface and the conducting material surface. This distance changes the mutual inductance of the circuits as the lift-off increases; the amplitude of the eddy current induces emf as the secondary coil decreases, which can result in the misinterpretation of the signals as flaws. At a significant lift-off, no detectable emf will be induced in the secondary coil due to the sample chosen.[81,87,88] This effect is particularly prominent when using sinusoidal excitations, which lose sensitivity beyond 5 mm.[89] Although it is not required to have a zero lift-off, it is imperative to try and maintain a consistent lift-off, since the variation in coupling between probe and test piece will

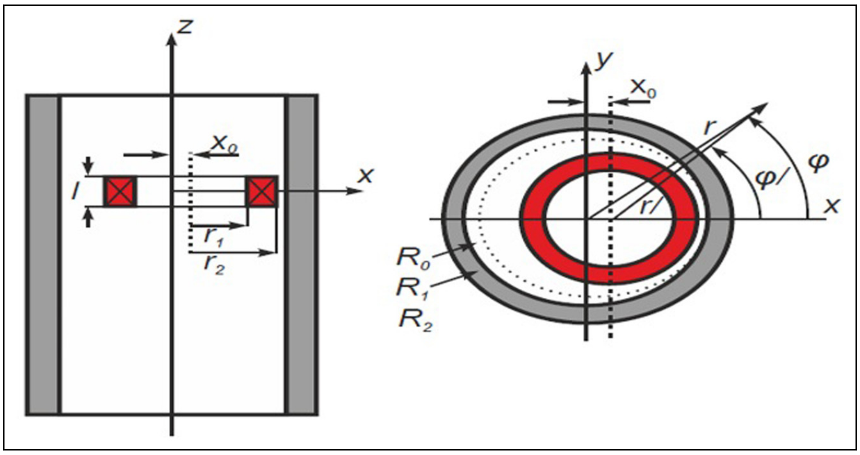

Figure 8. Wobble simulation: a bobbin coil in an offset position to a tube.[87]

significantly affect the received signal. Table 5 lists previous studies that have considered the lift-off issue.

Figure 8 illustrates the offset position of the tube inside the bobbin coils. Lift-off is explained using a coil whose axis is normal to the test piece. However, lift-off also occur when the test is conducted using encircling or bobbin probes. The vibration of the rod or the tube inside the probe generates noise which presents difficulties when inspections are conducted.[117]

There are methods for lift-off compensation when the eddy currents are used in order to detect cracks, and lift-off becomes an undesired variable. For instance, Yin et al.[100] researched dual excitation frequencies and coil design to minimize the lift-off effect. Research about processing the data was also conducted to minimize the lift-off effect. Lopez et al.[118] proposed the use of wavelets to remove the eddy current probe wobble noise from the steam generator's tubes. Reduction in the lift-off effect was also attempted by optimizing the coil design and sensor array.[119]

Tian et al.[101] had researched the reduction of lift-off effects via normalization techniques. The technique can be applied to the measurement of metal thickness beneath the non-conductive coatings and to the measurement of microstructure and strain/stress, where the output is highly sensitive to the lift-off effect. Table 5 illustrates previous studies that considered the lift-off issue.

Optimization of ECT probes design

According to the state of the art, the probability of detection techniques of eddy current techniques can be improved by the optimizing the probe design. In recent years, several studies have focused on optimization of the ECT probe design for defect detection. Rocha et al.[120] proposed an ECT probe design based on velocity-induced eddy currents to detect surface defects. Commercial simulation software was used for the optimization and design of the probe. Their experimental results confirmed that the proposed probe design was able to detect defects in the conductive materials where motion is involved.[120] A biorthogonal rectangular probe was developed by Zhang et al.[52] Simulation results showed the new biorthogonal rectangular probe has a lesser effect on the lift-off with higher sensitivity detection. Meanwhile, Cardoso et al.[121] optimized the sensor configuration in the eddy current probe design. A finite element modeling simulation was used to measure the accuracy detection of the probe design. Comparison of experimental and simulation date proved the accuracy of the proposed probe. Research by Rosado et al.[122] reported the influence of the geometrical parameters of an eddy currents planar probe in ECT. The findings showed that modifications of the studied parameters could substantially improve the probe performance. In a different study, Ghafari et al.[123] proposed a methodology for determining the optimal sensor parameters for ECT probe design. Simulation results showed the proposed sensor geometry improved the probe sensitivity to depth changes in a crack.

Chen and Miya[124] proposed ECT probes based on simplified detectability analysis method and a ring current model. The optimal probe designs are developed in view of the combinations of these excitation and pickup coils by comparing their detectabilities evaluated with the simplified analysis method. Aldrin et al.[125] presented a comprehensive approach to perform model-based inversion of crack characteristics using bolt hole eddy current techniques. Signal processing algorithms were developed for wide range of crack sizes and shapes, including mid-bore, corner and through thickness crack types. Inversion results for select mid-bore, through and corner crack specimens are presented, where sizing performance was found to be satisfactory in general but also depend on the size and location of the flaw. Table 6 summarizes previous studies on the optimization of the ECT probe design.

Application of artificial intelligent in eddy current

GMR sensor is used in ECT to pick up the MF in the presence of the defect. As the mutual inductance

Table 5. Review of lift-off compensation techniques.

Author	Technique software or hardware	Sensor type	Signal excitation	Sample type	Research Area
Fan et al.[90]	Model-based inversion algorithm	Air-core coil	Sinusoidal signal	Three plates of copper, aluminum and stainless steel	Lift-off elimination for model-based inversion method
Dziczkowski et al.[91]	Excremental/ mathematical model	Coil	Sine excitation at low frequencies is applied	Conductive material	To eliminate the lift-off between the coil and the specimen under test
Lu et al.[92]	Dodd and Deeds method	Coaxially arranged coils	Frequency sweeping	The metal plate	Reducing the lift-off effect on permeability measurement for magnetic plates from multi-frequency induction data
Ribeiro et al.[93]	Lift-off correction based on the spatial spectral behavior of eddy current	GMR	The probe excitation current was set to 100 mA at 5 kHz	A duralumin 2024 T3 plate	Increase the signal-to-noise ratio of measurements
Kral et al.[72]	Linear transformer model to investigate the effect of the lift-off	GMR sensor	Pulse signal	Metallic plate	Investigate the origin and the characteristics associated with the lift-off point of intersection (LOI)
Wu et al.[94]	Signal analysis base on multi-frequency phase signature	Coil	Sinusoidal signal with multi-frequency	Copper and aluminum plates	Presented a simple model for metal thickness measurement that is unaffected by lift-off effect to obtain the thickness
Yin and Xu[60]	Using peak frequencies of the sensor signal to estimate the thickness (h)	Bottom and top coils	Swap frequency	Aluminum plates	Designed a triple-coil sensor operating as two coil pairs and in a multi-frequency mode to measure plate thickness
Huang and Wu[95]	Relative magnetic flux changing rate (s)	Coil	Pulse signal and the square wave used as excitation current	Four 16Mn steel plates	Ferromagnetic object testing used to remove the lift-off effect without extra measurement of reference signals
Yu et al.[96]	Measure the defect dimension base on slope of the linear curve of the peak value	Hall sensor	Pulse signal	7075 and 2024 aluminum alloy plates	Reduce the lift-off noise for detection of defect depth or width
Zhu et al.[97]	Hough transform was used	Coil	Sinusoidal signal	Annealing copper plate	Investigate the lift-off effect in the normalized impedance plane
Lopes Ribeiro et al.[98]	The theory of the linear transformer	GMR	Sinusoidal excitation	Aluminum plates of type AL3105-H12	Measurement of the thickness of a metallic non-ferromagnetic plate
Tian and Sophian[99]	Normalization technique	Coil	Pulse signal	Two plates of aluminum	Minimize lift-off impact. It could be utilized for metal thickness measurement and for microstructure analysis
Yin et al.[100]	Analytical model that describes the inductance	Air-cored coil	Multi-frequency	Conducting plate	The phase signature of such a sensor is virtually lift-off independent
Tian et al.[101]	Analytical model based on the extended truncated region eigenfunction expansion	Hall sensor	Pulse signal	Plate conductor with arbitrary number of layers	Analyze LOI with respect to different PEC configurations and build

(Continued)

Table 5. (Continued)

Author	Technique software or hardware	Sensor type	Signal excitation	Sample type	Research Area
Wei et al.[102]	U-shaped ACFM system	Coils	The signal generator provides a 6 kHz sine voltage waveform signal	Mild steel sheet workpiece with a crack. The longitudinal	Determine an optimal lift-off value for a specific U-shaped ACFM system
Gotoh et al.[103]	The 3D edge-based hexahedral nonlinear FEM	A transverse type Hall element	The exciting frequency is set to 1 kHz	Nickel-coated steel plate	To inspect the thickness of nickel-layer on steel plate without the impact of lift-off
Lopes Ribeiro et al.[98]	A linear transformer model	GMR sensor	Sinusoidal signal	Aluminum plates	Measures the thickness of metallic
Gotoh et al.[104]	Electromagnetic acoustic transducer	Transducer coil	A 250 kHz sinusoidal burst current drives the EMAT coil	Steel plate	Suitable lift-off value for this specific EMAT system should be around 2 mm
Li et al.[105]	The relative variation of magnetic flux (s)	Coil	Pulse signal	Metal plate	Measurement of lift-off is extracted from the middle part of the PECT signal
Angani et al.[17]	Transient eddy current oscillations	Hall sensor	Pulses of the 50% duty cycle with the repetition rate of 2 s	Stainless steel plate	Eliminate the false indications due to the lift-off variations in the thickness measurement of the test material
Wang et al.[106]	The slope of the lift-off curve (SLOC) feature of the eddy current sensor (ECS)	Sensor coil	The working frequency (1 MHz)	Copper film	Immunity to lift-off variation
Wang et al.[107]	Pulsed eddy current (PEC) responses	Hall sensor	Pulse signal	Nonmagnetic plate	Study behaviors of lift-off point of intersection points due to a plate with varying conductivity and thickness
He et al.[108]	Principal component analysis and support vector machine	Coil	The excitation pulse used 19.6 V, 100 Hz	Two 3003vAl–Mn alloy plate	Defect-automated classification
Amineh et al.[109]	Blind deconvolution algorithm and a wavelet network inversion method	A tiny induction coil sensor	Alternating current	Metal surface	Lift-off evaluation and surface crack signal restoration
Hoshikawa and Koyama[110]	Improvements in probe design (h)	Tangential coil	Alternative current	Brass plate	To monitor the probe lift-off to avoid the probe not detecting flaws in the material
Lu et al.[111]	Multi-frequency inductance spectral data	Air-core coil	Sinusoidal signal	Metallic plates	Proposed a new index to compensate lift-off variation linked to the thickness. At different lift-offs, the accuracy of the thickness measurements proved to be more than 98%
Lu et al.[92,112]	Dodd and Deeds method	Air-core coil	Sinusoidal signal	Magnetic plates	Proposed a new modified permeability measurement technique for magnetic plates from multi-frequency induction data. The permeability error caused by lift-off can be reduced within 7.5%

(Continued)

Table 5. (Continued)

Author	Technique software or hardware	Sensor type	Signal excitation	Sample type	Research Area
Wen et al.[113]	Lift-off point of intersection has been applied to determine thickness or evaluate defects	Air-core coil	PEC	Metallic plates	The effective signal feature indicates that the frequency and amplitude at the LOI are decreased with sample thickness increasing. In addition, the frequency LOI can be used to measure the sample thickness functioning similarly to time domain LOI by monitoring the frequency and amplitude
Kral et al.[72] The time derivative of the	Linear transformer model magnetization curves obtained for different gaps between the excitation coil and the plate was proposed		Magnetoresistive sensor probe	Pulsed excitation	No ferromagnetic metallic plates
Yin et al.[114]	Simplified model related to thickness, conductivity and lift-offs	Air-core coil	Sinusoidal signal	Nonmagnetic metallic plate	Present the model with two independent parameters for a range of thickness, conductivity, and lift-offs
Wei et al.[115]	Design alternating current field measurement (ACFM) system	U-shaped probe	Sinusoidal signal	nonmagnetic metallic plate	Determine the optimum-induced frequency based on the signal acquisition and the measurement accuracy of an ACFM system
Fan et al.[116]	PEC spectral response to serve as robust features for thickness evaluation	Hall sensor	PEC	Nonmagnetic metallic plate	Propose to apply the phase of PEC spectral response from a Hall sensor rather than pickup coil–based probe to thickness measurement for the elimination of lift-off effect

GMR: giant magneto resistive; ACFM: alternating current filed measurement; FEM: finite element method; PECT: pulsed eddy current thermography.

between the coil and the specimen is sensitive to the lift-off, any changes in lift-off must be compensated for in order to achieve the accurate depth of defect measurements.

The fuzzy logic is instrumental for enhancing lift-off compensation. Artificial intelligent used is in many types of research in ECT. There are two common fuzzy inference methods: Mamdani's fuzzy inference method and Takagi–Sugeno–Kang, a method of fuzzy inference. The output from Mamdani fuzzy inference system (FIS) can be easily transformed into a linguistic form as the inference result before defuzzification.[135] The main difference between Mamdani-type FIS and Sugeno-type FIS resides in the way the crisp output is generated from the fuzzy inputs.[136] While Mamdani-type FIS uses the technique of defuzzification of a fuzzy output, Sugeno-type FIS uses weighted average to compute the crisp output,[137] so the Sugeno's output membership functions are either linear or constant, but Mamdani's inference expects the output membership functions to be fuzzy sets which are appropriate for comparing the peak of sensors. Based on artificial intelligent technology, a lot of research has been done by many researchers about ECT, as shown in Table 7.

Conclusion

This paper introduces an overview of the eddy current probes structure and error compensation techniques to obtain an ideal measuring depth of defect for the material under test. There are two techniques to sense the change in MF air coil and magnetoresistance sensor. Air coil is less sensitive at low frequency which required to inspect the surface of pipe and plate. This particular paper also reviews the manufacturer in the industry to produce the commercial probes for practical tube

Table 6. Summary previous studies on optimization of ECT probe design.

Authors	Research area	Optimization technique/ software tool	Observations
Betta et al.[126]	Optimized complex signals for ECT	Signals analyzed in transformed domains	The effect of suitable signal optimizations carried out to retrieve excitation frequencies linearly spaced in the skin depth domain instead of usual signals with a harmonic content linearly spaced in the frequency domain
Xiangchao and Feilu[127]	Optimization of PECT system for defect detection on aircraft-riveted structures	Phase-shift and logic-operation	The experimental results testify the availability of the optimized system and the necessity to optimize the PECT probe design parameters
Pereira and Clarke[128]	Modeling and design optimization of an eddy current sensor for superficial and sub-superficial crack detection in inconel claddings	Finite-element models were used as a tool for eddy current sensor design to optimize their geometry and operating frequency for detection of the defect	A good agreement was found between simulated and experimental results, showing that this is a robust strategy for special sensor design
Cardoso et al.[121]	Improved magnetic tunnel junctions design for the detection of superficial defects by eddy currents testing	Optimize the sensor configuration	The experimental results obtained showed very good agreement with the simulations for micron size defect detection
Karthik et al.[129]	Coil positioning for defect reconstruction in a steel plate	Genetic algorithm optimization method	The pancake exciting coil can read maximum voltage generated by the defect
Deabes et al.[130]	Optimized fuzzy image reconstruction algorithm for ECT systems	Fuzzy inference system (FIS)	The results show that the proposed optimized algorithm has high accuracy and promising features
Li et al.[131]	Multi-parametric indicator design for ECT sensor optimization used in oil transmission	A $L_9(3^4)$ orthogonal design	The experimental results indicated that the sensor structure optimized with the CFIECT could derive a greater sensitivity distribution and a better imaging reconstruction results
Vacher et al.[15]	Eddy current nondestructive testing with the giant magneto-impedance sensor	Fast semi-analytical models.	Improved the probe sensitivity performances at low frequencies and small size of defect detection
Chen and Miya[124]	A new approach for optimal design of ECT probes	Simplified detectability analysis method and a ring current model	The high performance of the new probe designs is assured
Thollon and Burais[132]	Geometrical optimization of sensors for eddy currents. Nondestructive testing and evaluation	Genetic algorithm	The optimized probe design showed high performance for cladding thickness measurement
Qi et al.[133]	Parameters optimization and nonlinearity analysis of grating eddy current displacement sensor using the neural network and genetic algorithm	Combined an artificial neural network (ANN) and a genetic algorithm (GA) for the sensor parameters optimization	The calculated nonlinearity error is 0.25%. These results show that the proposed method performs well for the parameters optimization of the GECDS
Huang et al.[27]	Design of an eddy current array probe for crack sizing in steam generator tubes	Numerical simulations	Experiments show that the proposed probe provides both a high detectability and a remarkable capability of reconstructing the shallow cracks of a tube
Rao et al.[134]	Optimization of eddy current probes for detection of garter springs in pressurized heavy water reactors	Two-dimensional finite element method is used to optimize eddy current probe design parameters	The eddy current probe can detect the displacement of garter springs

CFIECT: combination fuzzy index of the eddy current testing; GECDS: grating eddy current displacement sensor; ECT: eddy current testing.

Table 7. Intelligent technique in defect measuring.

Author	Proposed technique	Application	Remarks
Buck et al.[138]	ANN with statistical technique of PCA	Steam generator data in simultaneous measurement	High sensitivity
D'Angelo and Rampone[139]	Neural network	To classify the aerospace structure defects	The efficiency parameters were very high near to one
Preda and Hantila[140]	FEM/polarization method/NN method	Reconstruction of defect shapes with PEC	NN-based inversion approach produces an accurate and quick rebuilding of defect shape
Rosado et al.[141]	Digital signal processing (DSP) suggested in FPGA	Multi-frequency for ECT in real-time processing	Utilizing DSP to generate multi-frequency stimulus
Habibalahi et al.[142]	Neural network data fusion	Improving pulsed eddy current stress measurement	The ability of NN data fusion to enhance stress measurement reliability
He et al.[108]	PCA-based feature extraction methods (ANN)	Defect-automated classification	Defect can be classified satisfactorily when lift-off ranged from 0 to 1.4 mm
Rosado et al.[143]	An ANN using data obtained with FEM	To estimate the defect properties	The ANN has poor generalization ability outside the range
Babaei et al.[144]	FEM/ANN	Calculating the dimension of rectangular cracks	The results of NN are very guaranteeing to compare with targets
Peng[145]	Multilayer feed-forward error-back propagation neural network	Assessment of crack expansion direction	The estimation error by using the training BPNN presents to be less than 2° which meets the requirement
Rosado[146]	Artificial neural network and nonlinear regressions	Profile reconstruction and estimate depth and width of defect	Finite element model was applied to produce synthetic ECT data for some faulty scenarios
Postolache et al.[53]	ANN, including competitive neural network and multilayer perceptron/FEM	Estimation and classification the geometrical characteristic	The accuracy of defect classification was increased by using ANN
Zhang and Yang[147]	PSO algorithm/ANN-based forward model	Rebuilding of crack geometry from ECT signal	Reconstruct crack profile rapidly and accurately from ECT signals
Morabito and Versaci[148]	Fuzzy neural approach	To localizing hole in conducting plates	The fuzzy system is effective with a limited number of inputs
Guohou et al.[149]	Dempster–Shafer evidence theory/the fuzzy inference	Evaluate the defect in conductive structure	Using the D-S approach to determine the defect parameter
Upadhyaya et al.[150]	ANN and fuzzy logic technique	Flaw detection and tube defect parameter estimation	The estimation of tube defect parameters performed with a high accuracy
Fan et al.[151]	Both kernel principal component analysis (KPCA) and a support vector machine (SVM)	Study the influences of excitation frequency for a group of defects were revealed in terms of detection sensitivity, contrast between defect features and classification accuracy	Determine the optimal excitation frequency for a group of defects

ANN: artificial neural network; PCA: principal component analysis; FEM: finite element method; PEC: pulsed eddy current; FPGA: field-programmable gate array; ECT: eddy current testing; BPNN: back propagation neural network; PSO: particle swarm optimization.

inspection. In addition, compare the performance, detectability and the working principle of the bobbin probe, rotating probe and array probe for the pipe inspection was presented. The lift-off effects are the main factors affecting the ECT signal causing erroneous data interpretation. The lift-off effect is discussed in detail, ensuring that the measuring defect is right. Finally, briefly review different conventional and intelligent lift-off compensation.

Declaration of conflicting interests

The author(s) declared no potential conflicts of interest with respect to the research, authorship and/or publication of this article.

Funding

This work was supported by Huaiyin institute of Technology and University Malaysia Pahang under grant number RDU170379.

ORCID iD

Ahmed N AbdAlla https://orcid.org/0000-0002-8633-1833
Moneer A Faraj https://orcid.org/0000-0002-1945-9634

References

1. Kennedy JL. *Oil and gas pipeline fundamentals*. Houston, TX: PennWell Books, 1993.
2. Muñoz-Cobo JL, Chiva S, Essa MAAEA et al. Simulation of bubbly flow in vertical pipes by coupling Lagrangian and Eulerian models with 3D random walks models: validation with experimental data using multi-sensor conductivity probes and laser doppler anemometry. *Nucl Eng Des* 2012; 242: 285–299.
3. Giguere S. *Pulsed eddy-currents for corrosion detection*. Ottawa, ON, Canada: National Library of Canada [Bibliothèque nationale du Canada], 2000.
4. Betta G, Ferrigno L and Laracca M. GMR-based ECT instrument for detection and characterization of crack on a planar specimen: a hand-held solution. *IEEE T Instrum Meas* 2012; 61: 505–512.
5. Aguila-Muñoz J, Espina-Hernández J, Pérez-Benítez J et al. A magnetic perturbation GMR-based probe for the nondestructive evaluation of surface cracks in ferromagnetic steels. *NDT&E Int* 2016; 79: 132–141.
6. Lee J, Jun J, Kim J et al. Bobbin-type solid-state hall sensor array with high spatial resolution for cracks inspection in small-bore piping systems. *IEEE T Magn* 2012; 48: 3704–3707.
7. Postolache O, Ribeiro AL and Ramos HG. GMR array uniform eddy current probe for defect detection in conductive specimens. *Measurement* 2013; 46: 4369–4378.
8. Ye C, Huang Y, Udpa L et al. Novel rotating current probe with GMR array sensors for steam generate tube inspection. *IEEE Sens J* 2016; 16: 4995–5002.
9. Zeng Z, Deng Y, Liu X et al. EC-GMR data analysis for inspection of multilayer airframe structures. *IEEE T Magn* 2011; 47: 4745–4752.
10. Rifai D, Abdalla AN, Ali K et al. Giant magnetoresistance sensors: a review on structures and non-destructive eddy current testing applications. *Sensors* 2016; 16: 298.
11. Ali K, Abdalla ANA, Rifai D et al. A review on system development in eddy current testing and technique for defect classification and characterization. *IET Circ Device Syst* 2017; 11: 338–351.
12. García-Martín J, Gómez -Gil J and Vázquez-Sánchez E. Non-destructive techniques based on eddy current testing. *Sensors* 2011; 11: 2525–2565.
13. Khan AA. *Liquid penetrant and magnetic particle testing at level 2 (Series ITC)*. Vienna: IAEA, 2000.
14. Angani CS, Ramos HG, Ribeiro AL et al. Evaluation of transient eddy current oscillations response for thickness measurement of stainless steel plate. *Measurement* 2016; 90: 59–63.
15. Vacher F, Alves F and Gilles-Pascaud C. Eddy current nondestructive testing with giant magneto-impedance sensor. *NDT&E Int* 2007; 40: 439–442.
16. Faraj MA, Samsuri F and AbdAlla AN. Hybrid of eddy current probe based on permanent magnet and GMR sensor. *J Telecomm Electr Comp Eng* 2018; 10: 7–11.
17. Angani CS, Ramos HG, Ribeiro AL et al. Lift-off point of intersection feature in transient eddy-current oscillations method to detect thickness variation in stainless steel. *IEEE T Magn* 2016; 52: 1–8.
18. Sullivan S, Smith S and Sharp F. Simultaneous absolute and differential operation of eddy current bobbin probes for heat exchanger tube inspection. *Mater Eval* 2000; 58: 634–638.
19. Xu EX and Simkin J. Total and reduced magnetic vector potentials and electrical scalar potential for eddy current calculation. *IEEE T Magn* 2004; 40: 938–940.
20. Mao X and Lei Y. Analytical solutions to eddy current field excited by a probe coil near a conductive pipe. *NDT&E Int* 2013; 54: 69–74.
21. Xin J, Lei N, Udpa L et al. Rotating field eddy current probe with bobbin pickup coil for steam generator tubes inspection. *NDT&E Int* 2013; 54: 45–55.
22. Thirunavukkarasu S, Rao B, Jayakumar T et al. Techniques for processing remote field eddy current signals from bend regions of steam generator tubes of prototype fast breeder reactor. *Ann Nucl Energy* 2011; 38: 817–824.
23. Rifai D, Abdalla AN, Khamsah N, et al. Subsurface defects evaluation using eddy current testing. *Ind J Sci Technol* 2016; 9(9): 1–7.
24. Lafontaine G, Hardy F and Renaud J. X-Probe® ECT array: a high-speed replacement for rotating probes. In: *Proceeding of the 3rd international conference on NDE in relation to structural integrity for nuclear and pressurized components*, Seville, 14–16 November 2001, pp. 14–16. Brussels: European Commission.
25. Xiang P, Ramakrishnan S, Cai X et al. Automated analysis of rotating probe multi-frequency eddy current data from steam generator tubes. *Int J Appl Electrom* 2000; 12: 151–164.
26. Xin J, Lei N, Udpa L et al. Nondestructive inspection using rotating magnetic field eddy-current probe. *IEEE T Magn* 2011; 47: 1070–1073.
27. Huang H, Sakurai N, Takagi T et al. Design of an eddy-current array probe for crack sizing in steam generator tubes. *NDT&E Int* 2003; 36: 515–522.
28. Jella PK. *Automated compensation and classification algorithms for array probe eddy current nondestructive evaluation*. East Lansing, MI: Michigan State University, 2004.
29. Xin J. *Design and analysis of rotating field eddy current probe for tube inspection*. East Lansing, MI: Michigan State University, 2014.
30. Uchanin V and Najda V. *The development of eddy current technique for WWER steam generators inspection*. London: INTECH Open Access Publisher, 2011.
31. Udpa S and Moore P. Nondestructive testing handbook: electromagnetic testing. *ASNT*, 2004, https://www.asnt.org/MajorSiteSections/Publications/NDT_Handbooks.aspx
32. Ludwig R and Dai X-W. Numerical and analytical modeling of pulsed eddy currents in a conducting half-space. *IEEE T Magn* 1990; 26: 299–307.
33. Yang G, Tamburrino A, Udpa L et al. Pulsed eddy-current based giant magnetoresistive system for the inspection of aircraft structures. *IEEE T Magn* 2010; 46: 910–917.
34. Li X, Gao B, Woo WL et al. Quantitative surface crack evaluation based on eddy current pulsed thermography. *IEEE Sens J* 2017; 17: 412–421.
35. Bowler J and Johnson M. Pulsed eddy-current response to a conducting half-space. *IEEE T Magn* 1997; 33: 2258–2264.

36. Shokralla S, Morelli JE and Krause TW. Principal components analysis of multifrequency eddy current data used to measure pressure tube to calandria tube gap. *IEEE Sens J* 2016; 16: 3147–3154.
37. Harrison D. *Eddy-current inspection using hall sensors and transient excitation*. Defence Research Agency Technical Report no. DRA/SMC/TR941008, 1994. Farnborough: DRA.
38. Harrison D. Progress in the detection of cracks under installed fasteners using eddy currents. In: *AGARD Conference Proceedings on Impact of Emerging NDE-NDI Methods on Aircraft Design, Manufacture and Maintenance*. (No.462). 1990; 15: 1–8.
39. Giguere J, Lepine B, Dubois J et al. Detection of cracks beneath rivet heads via pulsed eddy current technique. In: *Proceedings of the AIP conference*, Albuquerque, NM, 3–6 February 2002, pp. 1968–1975. Melville, NY: AIP.
40. Di Iorio F. *Low field magnetic sensing with giant magneto resistive sensors*. Naples: Università degli Studi di Napoli Federico II, 2008.
41. Postolache O, Ramos HG and Ribeiro AL. Characterization of defects in aluminum plates using GMR probes and neural network signal processing In: *Proceedings of the XVI-IMEKO TC4 symposium*, Florence, 2008.
42. Reig C, Cubells-Beltran MD and Munoz DR. Magnetic field sensors based on giant magnetoresistance (GMR) technology: applications in electrical current sensing. *Sensors* 2009; 9: 7919–7942.
43. Deng Y and Liu X. Electromagnetic imaging methods for nondestructive evaluation applications. *Sensors* 2011; 11: 11774–11808.
44. Jander A, Smith C and Schneider R. Magnetoresistive sensors for nondestructive evaluation. In: *Proceedings of the nondestructive evaluation for health monitoring and diagnostics*, San Diego, CA, 2005, pp. 1–13. Bellingham WA: International Society for Optics and Photonics.
45. Li W, Yuan Xa Chen G et al. A feed-through ACFM probe with sensor array for pipe string cracks inspection. *NDT&E Int* 2014; 67: 17–23.
46. Du W, Nguyen H, Dutt A et al. Design of a GMR sensor array system for robotic pipe inspection. In: *Proceedings of the sensors, 2010 IEEE*, Kona, HI, 1–4 November 2010, pp. 2551–2554. New York: IEEE
47. Lebrun B, Jayet Y and Baboux J-C. Pulsed eddy current signal analysis: application to the experimental detection and characterization of deep flaws in highly conductive materials. *NDT&E Int* 1997; 30: 163–170.
48. Lebrun B, Jayet Y and Baboux JC. Pulsed eddy current application to the detection of deep cracks. *Mater Eval* 1995; 53: 1296–1300.
49. Kim J, Yang G, Udpa L et al. Classification of pulsed eddy current GMR data on aircraft structures. *NDT&E Int* 2010; 43: 141–144.
50. Tai CC, Rose JH and Moulder JC. Thickness and conductivity of metallic layers from pulsed eddy-current measurements. *Rev Sci Instrum* 1996; 67: 3965–3972.
51. D'Angelo G, Laracca M, Rampone S et al. Fast eddy current testing defect classification using Lissajous figures. *IEEE T Instrum Meas* 2018; 67: 821–830.
52. Zhang S, Tang J and Wu W. Calculation model for the induced voltage of pick-up coil excited by rectangular coil above conductive plate. In: *Proceedings of the IEEE international conference on mechatronics and automation (ICMA)*, Beijing, China, 2–5 August 2015, pp. 1805–1810. New York: IEEE.
53. Postolache O, Ramos HG and Ribeiro AL. Detection and characterization of defects using GMR probes and artificial neural networks. *Comp Stand Inter* 2011; 33: 191–200.
54. Yang G, Zeng Z, Deng Y et al. 3D EC-GMR sensor system for detection of subsurface defects at steel fastener sites. *NDT&E Int* 2012; 50: 20–28.
55. Yang G, Dib G, Udpa L et al. Rotating field EC-GMR sensor for crack detection at fastener site in layered structures. *IEEE Sens J* 2015; 15: 463–470.
56. Kim Y-J and Lee S-S. Eddy current probes of inclined coils for increased detectability of circumferential cracks in tubing. *NDT&E Int* 2012; 49: 77–82.
57. Paw J, Ali K, Hen C et al. Encircling probe with multi-excitation frequency signal for depth crack defect in eddy current testing. *J Fund Appl Sci* 2018; 10: 949–964.
58. Shim H-S, Choi MS, Lee DH et al. A prediction method for the general corrosion behavior of alloy 690 steam generator tube using eddy current testing. *Nucl Eng Des* 2016; 297: 26–31.
59. Ribeiro AL, Ramos HG and Postolache O. A simple forward direct problem solver for eddy current non-destructive inspection of aluminum plates using uniform field probes. *Measurement* 2012; 45: 213–217.
60. Yin W and Xu K. A novel triple-coil electromagnetic sensor for thickness measurement immune to lift-off variations. *IEEE T Instrum Meas* 2016; 65: 164–169.
61. Joubert PY, Vourc'h E and Thomas V. Experimental validation of an eddy current probe dedicated to the multi-frequency imaging of bore holes. *Sensor Actuat A-Phys* 2012; 185: 132–138.
62. Menezes R, Ribeiro AL and Ramos HG. Evaluation of crack depth using eddy current techniques with GMR-based probes. In: *Proceedings of the metrology for aerospace (Metroaerospace)*, Benevento, 4–5 June 2015, pp. 335–339. New York: IEEE.
63. Xie R, Chen D, Pan M et al. Fatigue crack length sizing using a novel flexible eddy current sensor array. *Sensors* 2015; 15: 32138–32151.
64. Suresh V, Abudhahir A and Daniel J. Development of magnetic flux leakage measuring system for detection of defect in small diameter steam generator tube. *Measurement* 2017; 95: 273–279.
65. Ye C, Huang Y, Udpa L et al. Differential sensor measurement with rotating current excitation for evaluating multilayer structures. *IEEE Sens J* 2016; 16: 782–789.
66. Lee KH, Baek MK and Park IH. Estimation of deep defect in ferromagnetic material by low frequency eddy current method. *IEEE T Magn* 2012; 48: 3965–3968.
67. Rifai D, Abdalla AN, Razali R et al. An eddy current testing platform system for pipe defect inspection based on an optimized eddy current technique probe design. *Sensors* 2017; 17: E579.
68. Abdalla A, Ali K, Paw J et al. A novel eddy current testing error compensation technique based on Mamdani-type fuzzy coupled differential and absolute probes. *Sensors* 2018; 18: E2108.
69. Liu Z, Tsukada K, Hanasaki K et al. Two-dimensional eddy current signal enhancement via multifrequency data fusion. *J Res Nondestruct Eval* 1999; 11: 165–177.
70. Aliouane S, Hassam M, Badidi Bouda A et al. Electromagnetic acoustic transducers (EMATs) design

evaluation of their performances. In: *Proceedings of the 15th world conference on NDT (WCNDT 2000)*, 2000, https://www.ndt.net/article/wcndt00/papers/idn591/idn591.htm
71. Bartels KA and Fisher JL. Multifrequency eddy current image processing techniques for nondestructive evaluation. In: *Proceedings of the international conference on image processing*, Washington, DC, 23–26 October 1995, p. 486. New York: IEEE.
72. Kral J, Smid R, Ramos HMG et al. The lift-off effect in eddy currents on thickness modeling and measurement. *IEEE T Instrum Meas* 2013; 62: 2043–2049.
73. Yadegari A, Moini R, Sadeghi S et al. Output signal prediction of an open-ended rectangular waveguide probe when scanning cracks at a non-zero lift-off. *NDT&E Int* 2010; 43: 1–7.
74. Ditchburn R, Burke S and Posada M. Eddy-current nondestructive inspection with thin spiral coils: long cracks in steel. *J Nondestruct Eval* 2003; 22: 63–77.
75. Thollon F, Lebrun B, Burais N et al. Numerical and experimental study of eddy current probes in NDT of structures with deep flaws. *NDT&E Int* 1995; 28: 97–102.
76. Owston C. Eddy-current testing at microwave frequencies. *Non-Destruct Test* 1969; 2: 193–196.
77. Ramos HG, Postolache O, Alegria FC et al. Using the skin effect to estimate cracks depths in metallic structures. In: *Proceedings of the instrumentation and measurement technology conference*, Singapore, 5–7 May 2009, pp. 1361–1366. New York: IEEE.
78. Postolache O, Ramos HG, Ribeiro AL et al. GMR based eddy current sensing probe for weld zone testing. In: *Proceedings of the sensors*, Christchurch, New Zealand, 25–28 October 2009, pp. 73–78. New York: IEEE.
79. Faraj MA, Samsuri F, Abdalla AN et al. Adaptive neuro-fuzzy inference system model based on the width and depth of the defect in an eddy current signal. *Appl Sci* 2017; 7: 668.
80. Faraj MA, Fahmi S, Damhuji R et al. Investigate of the effect of width defect on eddy current testing signals under different materials. *Ind J Sci Technol* 2017; 10: 1–5.
81. Mook G, Hesse O and Uchanin V. Deep penetrating eddy currents and probes. *Mater Test* 2007; 49: 258–264.
82. Placko D and Dufour I. Eddy current sensors for nondestructive inspection of graphite composite materials. In: *Proceedings of the industry applications society annual meeting conference*, Houston, TX, 4–9 October 1992, pp. 1676–1682. New York: IEEE.
83. Shull PJ. *Nondestructive evaluation: theory, techniques, and applications*. Boca Raton, FL: CRC Press, 2016.
84. Abbas S, Khan TM, Javaid SB et al. Low cost embedded hardware based multi-frequency eddy current testing system. In: *Proceedings of the international conference on intelligent systems engineering (ICISE)*, Islamabad, Pakistan, 15–17 January 2016, pp. 135–140. New York: IEEE.
85. Chen X and Lei Y. Electrical conductivity measurement of ferromagnetic metallic materials using pulsed eddy current method. *NDT&E Int* 2015; 75: 33–38.
86. Almeida G, Gonzalez J, Rosado L et al. Advances in NDT and materials characterization by eddy currents. *Procedia CIRP* 2013; 7: 359–364.
87. Cecco VS, Drunen GV and Sharp FL. Eddy current testing manual on eddy current method. *Atomic Energy of Canada Limited*, 1981; 1: 1–208.
88. Mokros SG, Underhill PR, Morelli J et al. Pulsed eddy current inspection of wall loss in steam generator trefoil broach supports. *Sensors* 2016; 17: 444–449.
89. Davies C. Dual mode coating thickness measuring instrument. *Google Patents*, 2004, https://patents.google.com/patent/US20020008511
90. Fan M, Cao B, Yang P et al. Elimination of liftoff effect using a model-based method for eddy current characterization of a plate. *NDT&E Int* 2015; 74: 66–71.
91. Dziczkowski L. Elimination of coil liftoff from eddy current measurements of conductivity. *IEEE Transactions on Instrumentation and Measurement* 2013; 62: 3301–3307.
92. Lu M, Zhu W, Yin L et al. Reducing the lift-off effect on permeability measurement for magnetic plates from multifrequency induction data. *IEEE T Instrum Meas* 2018; 67: 167–174.
93. Ribeiro AL, Alegria F, Postolache OA et al. Liftoff correction based on the spatial spectral behavior of eddy-current images. *IEEE T Instrum Meas* 2010; 59: 1362–1367.
94. Wu Y, Cao Z and Xu L. A simplified model for nondestructive thickness measurement immune to the lift-off effect. In: *Proceedings of the instrumentation and measurement technology conference (I2MTC)*, Binjiang, China, 10–12 May 2011, pp. 1–4. New York: IEEE.
95. Huang C and Wu X. Probe lift-off compensation method for pulsed eddy current thickness measurement. In: *Proceedings of 2014 3rd Asia-Pacific conference on antennas and propagation*, Harbin, China, 26–29 July 2014, pp. 937–939. New York: IEEE.
96. Yu Y, Yan Y, Wang F et al. An approach to reduce lift-off noise in pulsed eddy current nondestructive technology. *NDT&E Int* 2014; 63: 1–6.
97. Zhu W-l, Shen H-x and Chen W-x. New method for suppressing lift-off effects based on Hough transform. In: *Proceedings of the international conference on measuring technology and mechatronics automation*, Hunan, China, 11–12 April 2009, pp. 653–656. New York: IEEE.
98. Lopes Ribeiro A, Ramos HG and Couto Arez J. Liftoff insensitive thickness measurement of aluminum plates using harmonic eddy current excitation and a GMR sensor. *Measurement* 2012; 45: 2246–2253.
99. Tian GY and Sophian A. Reduction of lift-off effects for pulsed eddy current NDT. *NDT&E Int* 2005; 38: 319–324.
100. Yin W, Binns R, Dickinson SJ et al. Analysis of the lift-off effect of phase spectra for eddy current sensors. *IEEE T Instrum Meas* 2007; 56: 2775–2781.
101. Tian GY, Li Y and Mandache C. Study of lift-off invariance for pulsed eddy-current signals. *IEEE T Magn* 2009; 45: 184–191.
102. Wei L, Guoming C, Xiaokang Y et al. Analysis of the lift-off effect of a U-shaped ACFM system. *NDT&E Int* 2013; 53: 31–35.
103. Gotoh Y, Matsuoka A and Takahashi N. Electromagnetic inspection technique of thickness of nickel-layer on steel plate without influence of lift-off between steel and inspection probe. *IEEE T Magn* 2011; 47: 950–953.
104. Huang S, Zhao W, Zhang Y et al. Study on the lift-off effect of EMAT. *Sensor Actuat A-Phys* 2009; 153: 218–221.
105. Li J, Wu X, Zhang Q et al. Measurement of lift-off using the relative variation of magnetic flux in pulsed eddy current testing. *NDT&E Int* 2015; 75: 57–64.

106. Wang H, Li W and Feng Z. Noncontact thickness measurement of metal films using eddy-current sensors immune to distance variation. *IEEE T Instrum Meas* 2015; 64: 2557–2564.
107. Fan M, Cao B, Tian G et al. Thickness measurement using liftoff point of intersection in pulsed eddy current responses for elimination of liftoff effect. *Sensor Actuat A-Phys* 2016; 251: 66–74.
108. He Y, Pan M, Chen D et al. PEC defect automated classification in aircraft multi-ply structures with interlayer gaps and lift-offs. *NDT&E Int* 2013; 53: 39–46.
109. Amineh RK, Ravan M, Sadeghi SH et al. Removal of probe liftoff effects on crack detection and sizing in metals by the AC field measurement technique. *IEEE T Magn* 2008; 44: 2066–2073.
110. Hoshikawa H and Koyama K. A new eddy current surface probe without lift-off noise. In: *Proceedings of the 10th APCNDT*, Brisbane, 2001, https://www.ndt.net/article/apcndt01/papers/224/224.htm
111. Lu M, Yin L, Peyton AJ et al. A novel compensation algorithm for thickness measurement immune to lift-off variations using eddy current method. *IEEE T Instrum Meas* 2016; 65: 2773–2779.
112. Lu M, Xu H, Zhu W et al. Conductivity lift-off invariance and measurement of permeability for ferrite metallic plates. *NDT&E Int* 2018; 95: 36–44.
113. Wen D, Fan M, Cao B et al. Lift-off point of intersection in spectral pulsed eddy current signals for thickness measurement. *IEEE Sens Let* 2018; 2: 1–4.
114. Yin W, Peyton AJ and Dickinson SJ. Simultaneous measurement of distance and thickness of a thin metal plate with an electromagnetic sensor using a simplified model. *IEEE Sensors Letters* 2004; 53: 1335–1338.
115. Wei L, Guoming C, Wenyan L et al. Analysis of the inducing frequency of a U-shaped ACFM system. *NDT&E Int* 2011; 44: 324–328.
116. Fan M, Cao B, Sunny AI et al. Pulsed eddy current thickness measurement using phase features immune to liftoff effect. *NDT&E Int* 2017; 86: 123–131.
117. Theodoulidis T. Analytical modeling of wobble in eddy current tube testing with bobbin coils. *J Res Nondestruct Eval* 2002; 14: 111–126.
118. Lopez LANM, Ting DKS and Upadhyaya BR. Removing eddy-current probe wobble noise from steam generator tubes testing using wavelet transform. *Prog Nucl Energ* 2008; 50: 828–835.
119. Shu L, Songling H, Wei Z et al. Improved immunity to lift-off effect in pulsed eddy current testing with two-stage differential probes. *Russ J Nondestruct Test* 2008; 44: 138–144.
120. Rocha TJ, Ramos HG, Ribeiro AL et al. Magnetic sensors assessment in velocity induced eddy current testing. *Sensor Actuat A-Phys* 2015; 228: 55–61.
121. Cardoso FA, Rosado LS, Franco F et al. Improved magnetic tunnel junctions design for the detection of superficial defects by eddy currents testing. *IEEE T Magn* 2014; 50: 1–4.
122. Rosado LS, Cardoso FA, Cardoso S et al. Eddy currents testing probe with magneto-resistive sensors and differential measurement. *Sensor Actuat A-Phys* 2014; 212: 58–67.
123. Ghafari E, Costa H and Júlio E. RSM-based model to predict the performance of self-compacting UHPC reinforced with hybrid steel micro-fibers. *Constr Build Mater* 2014; 66: 375–383.
124. Chen Z and Miya K. A new approach for optimal design of eddy current testing probes. *J Nondestruct Eval* 1998; 17: 105–116.
125. Aldrin JC, Sabbagh HA, Zhao L et al. Model-based inverse methods for sizing cracks of varying shape and location in bolt-hole eddy current (BHEC) inspections. In: *Proceedings of the AIP conference*, AIP Publishing, https://aip.scitation.org/doi/pdf/10.1063/1.4940557
126. Betta G, Ferrigno L, Laracca M et al. Optimized complex signals for eddy current testing. In: *Proceedings of the instrumentation and measurement technology conference (I2MTC)*, Montevideo, Uruguay, 12–15 May 2014, pp. 1120–1125. New York: IEEE.
127. Xiangchao H and Feilu L. Optimization of PECT system for defect detection on aircraft riveted structures. In: *Proceedings of the 2011 international conference on computer science and network technology (ICCSNT)*, Harbin, China, 24–26 December 2011, pp. 996–999. New York: IEEE.
128. Pereira D and Clarke TG. Modeling and design optimization of an eddy current sensor for superficial and subsuperficial crack detection in inconel claddings. *IEEE Sens J* 2015; 15: 1287–1292.
129. Karthik VU, Mathialakan T, Jayakumar P et al. Coil positioning for defect reconstruction in a steel plate. In: *Proceedings of the 31st international review of progress in applied computational electromagnetics (ACES)*, Williamsburg, VA, 22–26 March 2015, pp. 1–2. New York: IEEE.
130. Deabes WA, Amin HH and Abdelrahman M. Optimized fuzzy image reconstruction algorithm for ECT systems. In: *Proceedings of the IEEE international conference on fuzzy systems (FUZZ-IEEE)*, Vancouver, BC, Canada, 24–29 July 2016, pp. 1209–1215. New York: IEEE.
131. Li N, Cao M, He C et al. A multi-parametric indicator design for ECT sensor optimization used in oil transmission. *Sensors* 2016; 17: 2074–2088.
132. Thollon F and Burais N. Geometrical optimization of sensors for eddy currents: non destructive testing and evaluation. *IEEE T Magn* 1995; 31: 2026–2031.
133. Qi H-l Zhao H, Liu W-w et al. Parameters optimization and nonlinearity analysis of grating eddy current displacement sensor using neural network and genetic algorithm. *J Zhejiang Univ-Sc A* 2009; 10: 1205–1212.
134. Rao BPC, Shyamsunder MT, Bhattacharya DK et al. Optimization of eddy-current probes for detection of garter springs in pressurized heavy water reactors. *Nucl Technol* 1990; 90: 389–393.
135. Mamdani E and Assilian S. An experiment in linguistic synthesis with a fuzzy logic controller. *Int J Hum-Comput St* 1999; 51: 135–147.
136. Blej M and Azizi M. Comparison of Mamdani-type and Sugeno-type fuzzy inference systems for fuzzy real time scheduling. *Int J Appl Eng Res* 2016; 11: 11071–11075.
137. Hamam A and Georganas ND. A comparison of Mamdani and Sugeno fuzzy inference systems for evaluating the quality of experience of Hapto-audio-visual applications. In: *Proceedings of the IEEE international workshop on Haptic audio visual environments and games*, Ottawa, ON, Canada, 18–19 October 2008, pp. 87–92. New York: IEEE.

138. Buck JA, Underhill PR, Morelli JE et al. Simultaneous multiparameter measurement in pulsed eddy current steam generator data using artificial neural networks. *IEEE T Instrum Meas* 2016; 65: 672–679.
139. D'Angelo G and Rampone S. Shape-based defect classification for non destructive testing. In: *Proceedings of the metrology for aerospace (Metroaerospace)*, Benevento, 4–5 June 2015, pp. 406–410. New York: IEEE.
140. Preda G and Hantila FI. Nonlinear integral formulation and neural network-based solution for reconstruction of deep defects with pulse eddy currents. *IEEE T Magn* 2014; 50: 113–116.
141. Rosado LS, Ramos PM and Piedade M. Real-time processing of multifrequency eddy currents testing signals: design, implementation, and evaluation. *IEEE T Instrum Meas* 2014; 63: 1262–1271.
142. Habibalahi A, Moghari MD, Samadian K et al. Improving pulse eddy current and ultrasonic testing stress measurement accuracy using neural network data fusion. *IET Sci Meas Technol* 2015; 9: 514–521.
143. Rosado LS, Janeiro FM, Ramos PM et al. Defect characterization with eddy current testing using nonlinear-regression feature extraction and artificial neural networks. *IEEE T Instrum Meas* 2013; 62: 1207–1214.
144. Babaei A, Suratgar AA and Salemi AH. Dimension estimation of rectangular cracks using impedance changes of the eddy current probe with a neural network. *J Appl Res Technol* 2013; 11: 397–401.
145. Peng X. Eddy current crack extension direction evaluation based on neural network. In: *Proceedings of the sensors*, Taipei, Taiwan, 28–31 October 2012, pp. 1–4. New York: IEEE.
146. Rosado L, Janeiro FM, Ramos PM et al. Eddy currents testing defect characterization based on non-linear regressions and artificial neural networks. In: *Proceedings of the instrumentation and measurement technology conference (I2MTC)*, Graz, 13–16 May 2012, pp. 2419–2424. New York: IEEE.
147. Zhang S and Yang H. Inversion of eddy current NDE signals using artificial neural network based forward model and particle swarm optimization algorithm. In: *Proceedings of the international conference on information and automation (ICIA'09)*, Macau, China, 22–24 June 2009, pp. 1314–1319. New York: IEEE.
148. Morabito E and Versaci M. A fuzzy neural approach to localizing holes in conducting plates. *IEEE T Magn* 2001; 37: 3534–3537.
149. Guohou L, Pingjie H, Peihua C et al. Application of multi-sensor data fusion in defects evaluation based on Dempster-Shafer theory. In: *Proceedings of the instrumentation and measurement technology conference (I2MTC)*, Binjiang, China, 10–12 May 2011, pp. 1–5. New York: IEEE.
150. Upadhyaya B, Yan W, Behravesh M et al. Development of a diagnostic expert system for eddy current data analysis using applied artificial intelligence methods. *Nucl Eng Des* 1999; 193: 1–11.
151. Fan M, Wang Q, Cao B et al. Frequency optimization for enhancement of surface defect classification using the eddy current technique. *Sensors* 2016; 16: E649.